Development 134, 3449-3460 (2007) doi:10.1242/dev.003095

Molecularly and temporally separable lineages form the hindbrain roof plate and contribute differentially to the choroid plexus

Nina L. Hunter and Susan M. Dymecki*

Both hindbrain roof plate epithelium (hRPe) and hindbrain choroid plexus epithelium (hCPe) produce morphogens and growth factors essential for proper hindbrain development. Despite their importance, little is known about how these essential structures develop. Recent genetic fate maps indicate that hRPe and hCPe descend from the same pool of dorsal neuroectodermal progenitor cells of the rhombic lip. A linear developmental progression has been assumed, with the rhombic lip producing non-mitotic hRPe, and seemingly uniform hRPe transforming into hCPe. Here, we show that hRPe is not uniform but rather comprises three spatiotemporal fields, which differ in organization, proliferative state, order of emergence from the rhombic lip, and molecular profile of either the constituent hRPe cells themselves and/or their parental progenitors. Only two fields contribute to hCPe. We also present evidence for an hCPe contribution directly by the rhombic lip at late embryonic stages when hRPe is no longer present; indeed, the production interval for hCPe by the rhombic lip is surprisingly extensive. Further, we show that the hCPe lineage appears to be unique among the varied rhombic lip-derived lineages in its proliferative response to constitutively active Notch1 signaling. Collectively, these findings provide a new platform for investigating hRPe and hCPe as neural organizing centers and provide support for the model that they are themselves patterned structures that might be capable of influencing neural development along multiple spatial and temporal axes.

KEY WORDS: Roof plate, Neural patterning, Choroid plexus, Genetic fate map, Inducible recombinases, Mouse

INTRODUCTION

Roof plate epithelium (RPe), via the secretion of patterning signals and growth factors, induces adjacent neuroectoderm to produce specific neuron subtypes (Lee et al., 2000; Lee and Jessell, 1999). In addition to patterning adjacent neuroectoderm, RPe derives from neuroectoderm (Awatramani et al., 2003; Landsberg et al., 2005) – specifically, from cells situated most laterally in the neural plate, which ultimately come to reside in the dorsal midline following transformation of the neural plate into the neural tube. In most anteroposterior (AP) regions of the neural tube, RPe thus appears as a morphologically distinct strip of cells at the dorsal midline (Fig. 1D). At the level of the hindbrain, however, RPe becomes an expansive dorsolateral sheet of cells. This is because closure of the neural plate to form a tube is transient in the hindbrain [occurring at around embryonic day (E)9]; instead of remaining closed at the dorsal midline as a tube, the edges of the hindbrain neural plate flare out laterally as the hindbrain flexes (Fig. 1A,B), with the RPe needing to tent over an expansive fourth ventricle (4v) (Fig. 1A-C). Regardless of whether RPe is a large sheet of cells, as in the hindbrain (hRPe, Fig. 1A,B), or a thin midline strip, as in other brain regions (RPe, Fig. 1D), it secretes morphogens crucial for neural tube patterning along the dorsoventral (DV) axis; for example, members of the bone morphogenetic protein (BMP) family (Chizhikov and Millen, 2004b).

Differentiation of RPe from neuroectoderm requires signals from neighboring epidermal ectoderm (Lee et al., 2000; Lee and Jessell, 1999; Liem, Jr et al., 1995). An initial defining feature of RPe and its progenitor cells is the expression of Lmx1a, a LIM-homeodomain transcription factor (Chizhikov and Millen, 2004b; Millonig et al., 2000). In spinal cord, RPe formation requires Lmx1a (Chizhikov and Millen, 2004a; Millen et al., 2004; Millonig et al., 2000); however, in the hindbrain, only certain AP regions of the hRPe are lost in the absence of Lmx1a (Chizhikov et al., 2006; Manzanares and Krumlauf, 2000; Millonig et al., 2000), hinting at possible molecular heterogeneity within the hRPe. Consistent with such heterogeneity, we have shown previously that hRPe is segmented along the AP axis such that hRPe derived from different rhombomeres (different AP levels) do not intermix (Awatramani et al., 2003) – a contrast to floor plate cells, the ventral counterpart of the roof plate, where extensive mixing occurs among cells derived from different rhombomeres (Fraser et al., 1990). The hRPe, as a result of these AP variations, might have the capacity to influence neural patterning along the AP as well as the DV axis.

A finding that further distinguishes hRPe, for example from spinal cord RPe, is its proposed generation of hindbrain choroid plexus epithelium (hCPe), a ribbon-like cuboidal epithelium that produces cerebrospinal fluid (CSF) and serves as the blood-CSF barrier (Redzic et al., 2005; Segal, 2000). Recent genetic fate maps suggest that the hCPe (a late-embryonic/adult structure suspending into the 4v) and the hRPe (an early/transient structure tenting over the 4v) descend from a common progenitor cell pool comprising dorsal-most neuroectodermal territory referred to as the rhombic lip (Fig. 1A,B) (Awatramani et al., 2003; Landsberg et al., 2005). Furthermore, hCPe, like hRPe, appears to comprise lineage-restricted compartments (Awatramani et al., 2003). A linear progression in development has been assumed, with the rhombic lip producing non-mitotic hRPe, and hRPe transforming into the more expansive hCPe (Thomas and Dziadek, 1993; Wilting and Christ, 1989) without cell gain (Dziegielewska et al., 2001; Kappers, 1955; Sturrock, 1979). The enormous increase in surface area of hCPe

Department of Genetics, Harvard Medical School, 77 Avenue Louis Pasteur, Boston, MA 02115, USA.

*Author for correspondence (e-mail: dymecki@genetics.med.harvard.edu)

Accepted 20 July 2007

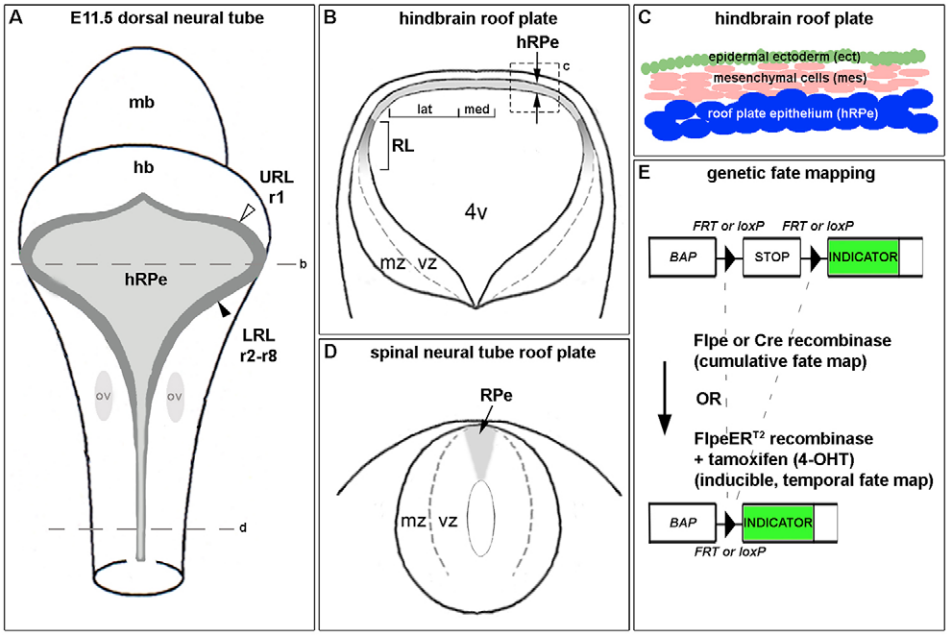

Fig. 1. Roof plate epithelium in the hindbrain. (**A**) Cartoon of a dorsal view of the neural tube (E11.5); neuroepithelium of the rhombic lip is dark gray and hindbrain roof plate epithelium (hRPe) is light gray. The rhombic lip in rhombomere 1 (r1) is the cerebellar or upper rhombic lip (URL, white arrowhead); that within r2-r8 is the hindbrain or lower rhombic lip (LRL, black arrowhead). Broken line marked by 'b' indicates the level of the idealized transverse section shown in B and the section plane in subsequent figures. Broken line marked by 'd' indicates the axial level of idealized transverse section through the spinal neural tube depicted in **D**. (**B**) Vertical bracket demarcates the dorsoventral (DV) region of the rhombic lip (RL); horizontal brackets demarcate medially (med) versus laterally (lat) located hRPe (relevant to subsequent figures). Boxed area (c) is further schematized in **C**. (**E**) Schematic of cumulative and inducible (temporal) fate mapping. A broadly active promoter (BAP) drives expression of an indicator transgene containing either an *FRT*- or *lox*P-flanked stop cassette followed by a sequence encoding a reporter molecule that serves as a lineage tracer. Transcription of the reporter is prevented by the stop cassette (top); excision by Flpe or Cre (or following FlpeER^{T2}-mediated recombination in the presence of tamoxifen), permits reporter transcription (bottom). mb, midbrain; hb, hindbrain; ov, otic vesicle; 4v, fourth ventricle; vz, ventricular zone; mz, post-mitotic mantle zone; ect, epidermal ectoderm; mes, mesenchyme; RPe, roof plate epithelium.

versus hRPe has been viewed as arising solely through changes in cell shape – densely packed pseudostratified hRPe spreads out to form the simple cuboidal hCPe (Dohrmann, 1970). In addition to producing CSF, the hCPe is thought to play a patterning role during late embryogenesis via its secretion of morphogens and growth factors, including BMPs and fibroblast growth factors (Emerich et al., 2005).

Here, we extend our understanding of how hRPe and hCPe develop. We show that hRPe comprises three molecularly distinct spatiotemporal fields with only two appearing to contribute to hCPe. Further, we show that hCPe receives contributions directly from the rhombic lip at late embryonic stages when hRPe seems no longer present. This supports a model of hCPe development in which transformation through an hRPe intermediate is not required and counters the view that hCPe formation is strictly a conservative process. Further, we show that the hCPe lineage appears to be unique among rhombic lip-derived lineages in that it proliferates in response to ligand-independent activation of the Notch1 pathway. Together, these findings offer a new platform for investigating development, function, aging and regeneration of the hRPe and hCPe, and support the model that they are themselves patterned, segmental structures, perhaps capable of influencing neural diversity along multiple spatial and temporal axes.

MATERIALS AND METHODS

Mouse strains

Mouse lines include: *Gdf7::cre* (Lee et al., 2000); *En1::cre* (*En1-cre*) (Kimmel et al., 2000); *Egr2::cre* (Voiculescu et al., 2000); *Rse2::cre* (*Rse2* refers to a rhombomere 2-specific enhancer) (Awatramani et al., 2003); *Wnt1::cre* (Chai et al., 2000); *Math1::cre* (*Math1* is also known as *Atoh1* – Mouse Genome Informatics) (Matei et al., 2005); *Wnt1::Flpe* (Awatramani et al., 2003); *Wnt1::FlpeER^{T2}* (Hunter et al., 2005); *R26R* (Soriano, 1999); *R26::FRAP* (Awatramani et al., 2001); *RC::Fa* (R. Awatramani, A. F. Farago and S.M.D., unpublished; Flp-responsive nβgal indicator); *RC::PFttc* (A. F. Farago and S.M.D., unpublished; Cre-responsive nβgal indicator); *RC::PFwe* (Farago et al., 2006); *R26::stop-Notch1-ICD::IRES-nGFP* (Murtaugh et al., 2003).

Bromodeoxyuridine (BrdU) injections

For each developmental stage, pregnant females were injected intraperitoneally with 30 μg of BrdU (Roche) per gram of body weight.

Tamoxifen (TAM) administration

Intraperitoneal TAM (Sigma) injections were given as follows: injection time point to harvest time point = dose per 40 g body weight. E7.5 to E11.5 = 6 mg; E8.5 to E11.5 = 7 mg; E9.5 to E11.5 = 8 mg; E7.5 to E16.5 = 5 mg; E8.5 to E16.5 = 6 mg; E9.5 to E16.5 = 7 mg; E10.5 to E16.5 = 7 mg; E11.5 to E16.5 = 8 mg; E12.5 to E16.5 = 9 mg; E13.5 to E16.5 = 10 mg; E14.5 to E16.5 = 11 mg; E15.5 to E16.5 = 12 mg (Hunter et al., 2005).

In situ hybridization (ISH), X-gal and alkaline phosphatase (PLAP) histochemistry

Embryos were prepared for cryosection (30 μm) and mRNA ISH (Hunter et al., 2005). Riboprobes directed against the following mRNAs were used: *AP-2α* (GenBank 3983850, Open Biosystems), *Barhl1* (GenBank AI324745, Research Genetics), *Bmp7* (C. Cepko, Harvard Medical School, MA), *Br* (C. Tabin, Harvard Medical School, MA), *Gdf7* (K. Millen, University of Chicago, IL), *FlpeER^{T2}* (Hunter et al., 2005), *Kcne2* (C. Cepko), *Lmx1a* (K. Millen), *Math1* (m*Atoh1*) (GenBank BC010820, Open Biosystems), *Notch1* (C. Cepko), *Pax3* (C. Tabin), *Sox9* (C. Tabin), *Ttr* (C. Walsh, Harvard Medical School, MA), and *Wnt1* (A. McMahon, Harvard University, MA). Detection of βgal on whole tissue and sections was performed as described (Farago et al., 2006). Detection of PLAP followed established protocols (Hunter et al., 2005), except: slides were post-fixed in 4% PFA, dehydrated in methanol, cleared in benzyl alcohol:benzyl benzoate (1:2, Sigma) and rehydrated.

Immunodetection

For co-detection of either βgal and BrdU or GFP and BrdU, embryos were soaked in 30% sucrose/PBS for 3 hours at 4°C, embedded in OCT (Tissue-Tek), sectioned (30 μm), fixed in 4% PFA/PBS for 10 minutes, blocked in

5% goat serum and 0.1% Triton X-100/PBS (BB), incubated overnight with rabbit anti-βgal (MP Biomedicals, 1:5000) or rabbit anti-GFP (Molecular Probes, 1:5000) in BB at 4°C, incubated with goat anti-rabbit Cy2 (Jackson ImmunoResearch, 1:500) in BB for 3 hours at room temperature (RT), incubated overnight at 4°C with rat anti-BrdU (Serotec, 1:500) in BB, incubated with goat anti-rat Cy3 (Jackson ImmunoResearch, 1:500) in BB for 3 hours at RT, exposed to 1 μg/ml DAPI (Sigma), and mounted. For co-detection of βgal and Ki-67 or GFP and Ki-67, the above protocol was used except: embryos were fixed in 0.2% PFA for 3 hours prior to sucrose; combined primary antibodies rabbit anti-βgal and mouse anti-Ki-67 (BD PharMingen, 1:200) or rabbit anti-GFP and mouse anti-Ki-67 were incubated at 4°C; combined secondary antibodies anti-rabbit Cy2 and anti-mouse Cy3 (Jackson ImmunoResearch) were incubated at RT.

RESULTS

Distinct fields within the hindbrain roof plate

Recent genetic fate maps show that the mouse hRPe at ~E11 is comprised of lineage-restricted compartments along the AP dimension (Awatramani et al., 2003) – a contrast to the AP cell dispersion characterizing floor plate (Fraser et al., 1990). Here, we re-examined our earlier finding of hRPe segmentation using a genetic fate mapping indicator allele with improved sensitivity due to encoding a nuclear-localized βgal (nβgal) as lineage tracer (Farago et al., 2006). We coupled this new Cre-responsive nβgal indicator allele with recombinase transgene *Egr2::cre* (Voiculescu et al., 2000) to map hRPe emerging from rhombomeres 3 and 5 (r3 and r5). As predicted (Awatramani et al., 2003), nβgal-positive (nβgal+) cells were found in stripes in the lateral hRPe at ~E11.5, supporting the model that these cells develop in a segmental, lineage-restricted fashion (Fig. 2B, lat). Not predicted was our detection of a midline hRPe field harboring an admixture of cells derived from different rhombomeres – reminiscent of the cell dispersion reported for floor plate (Fig. 2B, med) (Fraser et al., 1990). Interestingly, this newly observed medial hRPe population appeared to disperse anteriorly to a greater extent than posteriorly [also seen when using an r2-specific Cre driver (*Rse2::cre*) (Awatramani et al., 2003), data not shown]; the basis for such differential cell movement is unknown.

Next, we examined whether compartments versus admixtures of hRPe cells were present earlier. At E9.5, we found AP mixing of nearly all hRPe cells (Fig. 2A). Together with the finding that hRPe arises from dorsal-most neuroectoderm within the rhombic lip (Awatramani et al., 2003; Landsberg et al., 2005), these results suggest a model whereby hRPe cells emerging from the rhombic lip at E9.5 mix along the AP axis, whereas hRPe cells emerging later constrain to AP compartments and reside laterally.

These two hRPe fields, defined by either compartmentalization or dispersion along the AP dimension, were also found to differ dorsoventrally. Using doubly transgenic *Wnt1::cre; Cre-responsive βgal indicator* mice to distinguish hRPe cells (βgal+) from neighboring mesenchyme and overlying epidermal ectoderm, we found that laterally located hRPe cells (Fig. 2C,G, laterally located green cells) segregate from overlying mesenchyme and epidermal ectoderm (Fig. 2C,G, and cartooned in Fig. 1C), whereas medially located hRPe cells (Fig. 2C,F, medially located green cells) disperse among mesenchymal cells (Fig. 2C, blue cells and Fig. 2F, red cells). Although this dispersion of medial hRPe among mesenchyme is reminiscent of some neural crest cells, we detected no expression of various neural crest markers [e.g. *AP-2α*, *Pax3* and *Sox9* (Chan, 2003; Zhao et al., 1997)] in these cells (see Fig. S1 in the supplementary material).

To determine whether hRPe cells in these two fields differed in their proliferative capacity, immunodetection of the nuclear antigen Ki-67 was performed: *Wnt1::cre; Cre-responsive βgal indicator* mice were used in order to distinguish, by βgal expression, hRPe cells from neighboring mesenchyme and epidermal ectoderm. hRPe at E9.5 showed co-localization of βgal and Ki-67 whether medially or laterally located (Fig. 2D,E, white arrowheads). By contrast, at E11.5, little co-labeling was observed, with an occasional cycling hRPe cell detected medially but only quiescent hRPe cells laterally (Fig. 2F,G). Thus, by E11.5, midline hRPe was becoming mitotically quiescent, whereas laterally located hRPe cells were quiescent immediately upon emerging from the rhombic lip (Fig. 2G, inset, white arrowhead).

Our data thus far suggest that, at E11.5, there are two distinct hRPe fields differing in adhesion properties and proliferative capacity: a lateral field of non-mitotic cells organized into lineage-restricted compartments versus a medial field of an admixture of cells from different axial levels of which a few are mitotic. Similarities between the medial hRPe field at E11.5 and earlier hRPe cells at E9.5 suggest a production sequence whereby medially located hRPe cells emerge from the rhombic lip prior to those situated laterally, with both populations having migrated dorsomedially from the rhombic lip. To address this suggested production sequence, we generated a temporal fate map of hRPe progenitors. We partnered with a Flp-responsive alkaline phosphatase (PLAP) indicator allele (Awatramani et al., 2001), an inducible version of Flpe recombinase [FlpeER^{T2} (Hunter et al., 2005)] expressed under the control of *Wnt1* regulatory elements (Fig. 1E). By activating FlpeER^{T2} at different stages with a single dose of tamoxifen (TAM), we were able to activate PLAP as a lineage tracer in temporally sequential cohorts of *Wnt1*-expressing progenitor cells in the rhombic lip and determine their fate within the E11.5 hRPe. In these experiments, PLAP activation occurred within the rhombic lip, as opposed to within the descendant cells themselves, because the latter do not express *Wnt1* or *FlpeER^{T2}* (Hunter et al., 2005), and because the half-life of FlpeER^{T2} is relatively short and thus does not perdure into descendant cells. Further, hRPe cells marked by PLAP probably emerge from the rhombic lip during an approximate 12 hour window, starting at around 12 hours post-TAM administration (Hunter et al., 2005).

Following E9.5 TAM administration, and therefore ~E10.0-E10.5 lineage tracer activation, we observed at E11.5 an abundance of PLAP+ cells throughout the lateral but not medial hRPe field (Fig. 2I). Following E7.5 TAM administration, and therefore ~E8.0-E8.5 lineage tracer activation, we detected at E11.5 scattered PLAP+ cells in both medial and lateral hRPe fields (Fig. 2H) – albeit few in number because the *Wnt1::FlpeER^{T2}* transgene (like endogenous *Wnt1*) is just beginning to be expressed at this early time point with little FlpeER^{T2} protein yet present. Although limited by both low *Wnt1* expression and dose of tamoxifen that can be given at this early time point, these findings nonetheless support a model whereby TAM administration at E7.5 triggers recombination events within rhombic lip cells at ~E8, with these cells subsequently undergoing asymmetric divisions – one set of daughter cells emerging dorsomedially from the rhombic lip to populate the medial hRPe field while the other set remains cycling in the rhombic lip to later give rise to progeny hRPe cells that situate laterally. In this model, generation of the medial hRPe field is largely complete by ~E10, after which progenitor cells of the rhombic lip give rise to lateral fields. Thus, medial-to-lateral position within the E11.5 hRPe probably corresponds to a temporal axis of cell production from the rhombic lip.

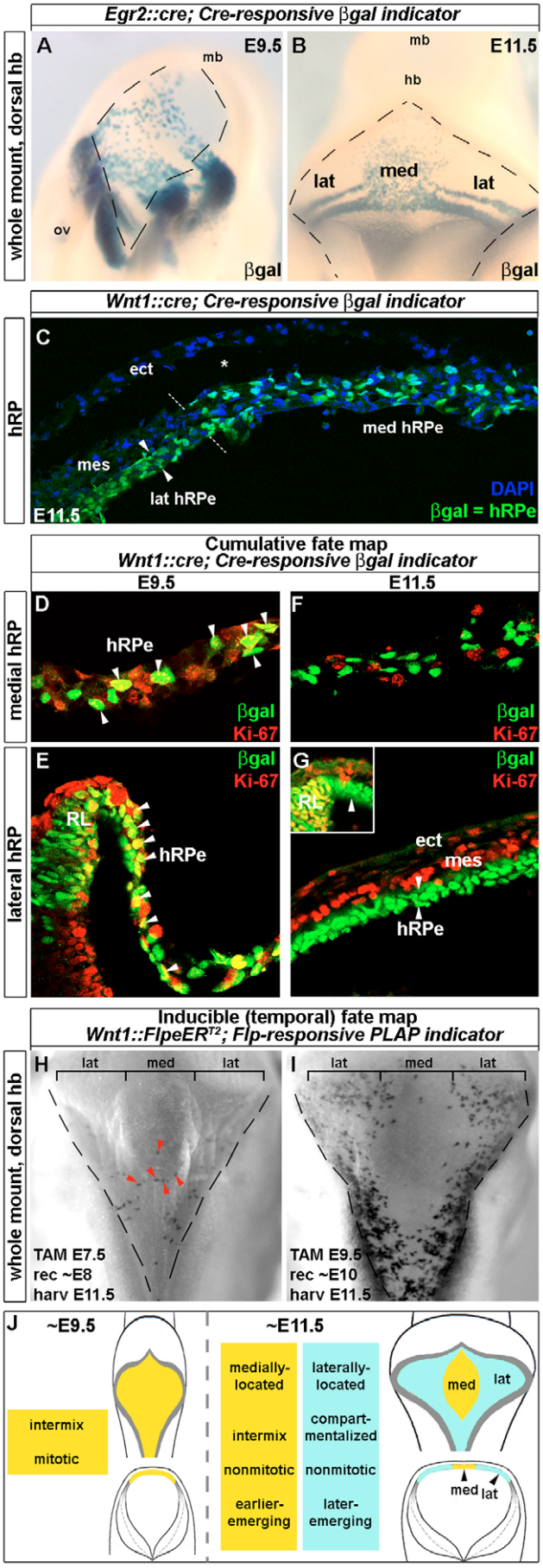

Fig. 2. Medial versus lateral roof plate cells differ in tissue organization, proliferative capacity and order of emergence from the rhombic lip. (**A**,**B**) Doubly transgenic embryos *Egr2::cre (r3/r5 cre allele); RC::PFwe (Cre-responsive βgal indicator allele)* X-gal-stained for βgal activity. Broken lines demarcate the rhombic lip. (A) At E9.5, hindbrain roof plate epithelium (hRPe) cells arising from different rhombomeres intermix anteriorly. (B) At E11.5, medially located (med) hRPe cells are an admixture from different rhombomeres, whereas laterally located (lat) hRPe cells are compartmentalized with respect to rhombomeric origin. (**C**) Transverse section through an E11.5 doubly transgenic *Wnt1::cre; Cre-responsive βgal indicator* embryo so as to distinguish hRPe cells by βgal activity (green); DAPI is shown in blue. Broken white line highlights the sharp border in tissue organization observed between laterally and medially located hRPe cells. Asterisk indicates a tear in the tissue, resulting in ectoderm cells situating away from mesenchymal cells. Arrowheads indicate laterally located hRPe that is segregated from overlying mesenchyme and epidermal ectoderm. (**D-G**) Transverse sections through a doubly transgenic *Wnt1::cre; Cre-responsive βgal indicator* embryo, with βgal expression (green by immunodetection) distinguishing rhombic lip and hRPe from mesenchyme and ectoderm; Ki-67 immunoreactivity is in red. Co-labeling was detected in both medially and laterally located hRPe at E9.5 (arrowheads, D,E), but largely absent in medially and laterally located hRPe at E11.5 (F and arrowheads in G). Inset in G shows proliferation (co-labeling) of rhombic lip cells; arrowhead demarcates non-mitotic laterally located hRPe. (**H**,**I**) Doubly transgenic *Wnt1::FlpeER^{T2}; R26::FRAP* embryos (E11.5) treated for PLAP histochemistry (cells marked by black precipitate). Broken lines demarcate the lower rhombic lip. Induction of recombination by tamoxifen (TAM) administration separates temporal cohorts of *Wnt1* (rhombic lip)-derived hRPe. (H) E7.5 TAM administration (~E8 recombination in the rhombic lip) resulted in labeled hRPe cells in both medial (med, red arrowheads) and lateral (lat) roof plate locations, albeit a modest number. (I) E9.5 TAM administration (~E10 recombination in the rhombic lip) resulted in labeled hRPe cells in only laterally located roof plate. (**J**) Summary schematic. At E9.5, hRPe cells intermix and are mitotic (yellow). At E11.5, two fields of hRPe are present: (1) cells that are medially located, dispersed and largely non-mitotic that emerged early from the rhombic lip (yellow) and (2) cells that are laterally located, compartmentalized along the anteroposterior (AP) and dorsoventral (DV) axes, are non-mitotic, and that emerged later from the rhombic lip (blue). mb, midbrain; hb, hindbrain; ov, otic vesicle; ect, epidermal ectoderm; mes, mesenchyme; rec, recombination time point; harv, harvest time point; RL, rhombic lip; TAM, tamoxifen.

Having uncovered two hRPe fields differing in position, tissue organization, proliferation and time of emergence from the rhombic lip, we asked whether the respective parental progenitor cells for each field differ molecularly, reflecting that different genetic programs might be involved in their production. *Wnt1* and *Wnt1::cre* were expressed in dorsal hindbrain neuroepithelium but not in hRPe or neighboring mesenchyme (see Fig. S2 in the supplementary material, and data not shown); cumulative fate mapping using doubly transgenic mice (*Wnt1::cre; Cre-responsive βgal indicator*) showed extensive cell marking throughout the entire hRPe at E11.5 (Fig. 3A-D and Fig. 2C-G). By contrast, *Gdf7* and *Gdf7::cre* expression in the rhombic lip began between ~E9.25 and E9.5, with Cre activity in *Gdf7::cre; Cre-responsive βgal indicator* mice first detectable at ~E9.5, presenting as βgal activity in the rhombic lip and lateral but not medial hRPe fields (Fig. 3E-H). Thus, cells constituting the medial hRPe field derive from progenitor cells that express *Wnt1* but not yet *Gdf7*, whereas cells of the lateral hRPe field derive from antecedents that expressed both.

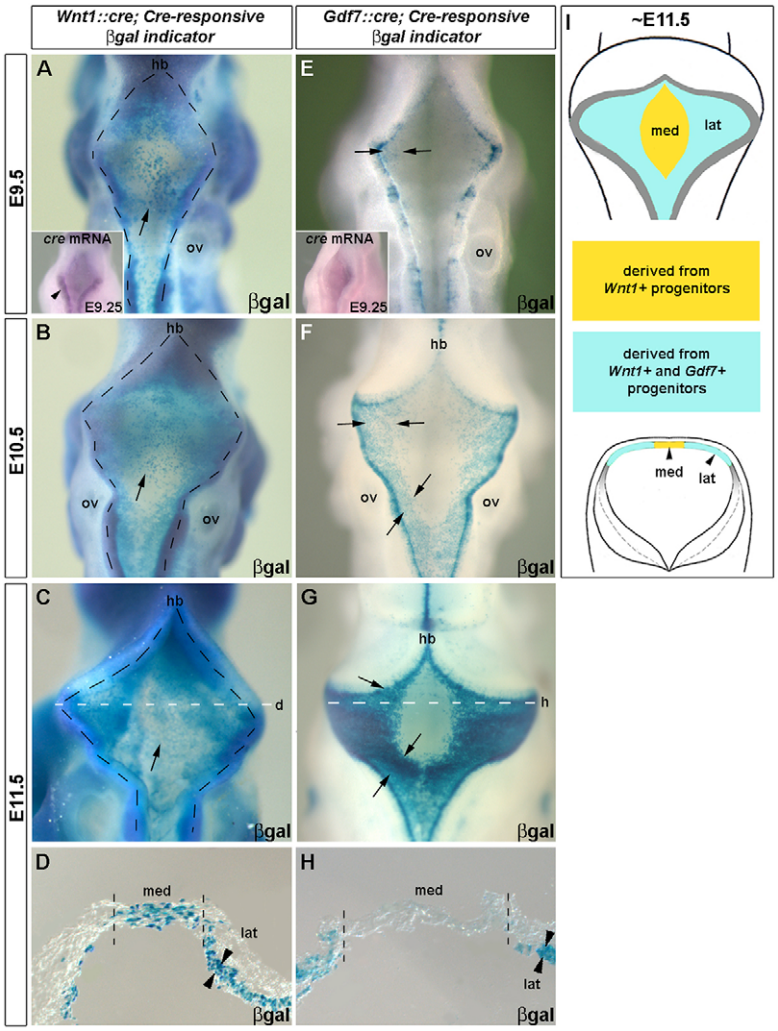

Fig. 3. A sequential change in progenitor-cell gene expression in the rhombic lip distinguishes laterally from medially fated roof plate cells. (**A-D**) Doubly transgenic *Wnt1::cre; Cre-responsive βgal indicator* embryos, with βgal detected by X-gal staining. (A-C) Dorsal whole-mount views showing βgal activity throughout the entire hindbrain roof plate epithelium (hRPe; arrows), both medially and laterally. Black broken lines demarcate the rhombic lip. Inset in A shows *cre* mRNA in the lower rhombic lip at ~E9.25 (arrowhead); *Wnt1* and *Wnt1::cre* are expressed in dorsal hindbrain neuroepithelium, but not in hRPe, from ~E8 onwards. (D) Transverse section taken at the rhombomeric level of the white broken line in C, revealing βgal+ hRPe cells medially (med) and laterally (lat). (**E-H**) Doubly transgenic *Gdf7::cre; R26R* embryos, with βgal detected by X-gal staining. (E-G) Dorsal whole-mount views showing βgal in laterally (arrows) but not medially located hRPe. Inset in E shows little to no *cre* mRNA in the rhombic lip at ~E9.25, with *Gdf7* and *cre* expression starting between ~E9.25 and E9.5. (H) Transverse section taken at the rhombomeric level of the white dashed line in G, revealing βgal+ hRPe cells laterally only (arrowheads). Black broken line demarcates the rhombic lip. (**I**) Schematic of hRPe fields at ~E11.5. Medially located hRPe (yellow) has a history of *Wnt1* expression, whereas laterally located hRPe (blue) has a history of *Wnt1* and *Gdf7* expression. ov, otic vesicle; hb, hindbrain; med, medial; lat, lateral.

R1-derived hRPe remains molecularly naïve until E13.5, lagging days behind that derived caudally

In addition to deriving from temporally and molecularly distinct progenitor cells of the rhombic lip, the two hRPe fields themselves differ in molecular expression. Lateral but not medial hRPe fields express genes such as *Bmp7*, *Gdf7*, *Lmx1a*, *Kcne2* [the latter encoding a potassium voltage-gated channel protein (Lundquist et al., 2006)] and transthyretin [*Ttr*, encoding the carrier protein for thyroid hormone (Harms et al., 1991; Herbert et al., 1986)] (Fig. 4A-F, and data not shown). The expression profiles of *Kcne2* and *Ttr* not only distinguish lateral from medial hRPe but also identify an unexpected AP subdivision within the lateral field (Fig. 4A-F). At E11.5, *Kcne2* and *Ttr* transcripts were detectable in lateral hRPe spanning axial levels r2-r8, but not in lateral hRPe territory situated at the level of r1 [the latter territory demarcated by βgal activity in *En1::cre* (*En1-cre*)*; Cre-responsive βgal indicator* mice (Machold and Fishell, 2005; Zervas et al., 2004)]. Thus, the hRPe at E11.5 appears divisible into at least three domains, shown in Fig. 4T: a medial field (yellow), an r2-r8 caudolateral field (light blue) and an r1 rostrolateral field (dark blue).

Given that a region of the hCPe appears to derive from r1 (*En1::cre* fate map in Fig. 4I,M,Q), we investigated at which time point r1-derived hRPe (Fig. 4T, field 3) or r1-derived hCPe become *Ttr*+ and *Kcne2*+. This occurs after ~E12.5 (Fig. 4L), ~3 days later than that observed for field 2 (Fig. 4B,E). Thus, although emerging simultaneously from the rhombic lip, lateral roof plate derivatives from r1 show a temporal lag in molecular fate as compared with those from r2-r8.

hRPe fields contribute differentially to choroid plexus epithelium

hRPe cells are thought to undergo shape changes beginning at ~E12 in order to form directly the entire hCPe (Lindeman et al., 1998). Having established that the hRPe is comprised of at least three fields distinguished in their spatial, temporal and molecular development, we sought to determine whether these differences correlate with cell fate with respect to hCPe. Previously, we have shown that the hCPe is a compartmentalized structure, with little mixing of hCPe cells that arise from different rhombomeres (Awatramani et al., 2003). Indeed, we observed this further in the present r1 (*En1::cre*) fate map of the hCPe (Fig. 4M,Q). Because areas of hCPe harboring an admixture of marked and unmarked cells were not observed, it seems unlikely that the medial hRPe (Fig. 4T, field 1) contributes substantially to hCPe. Because medial hRPe cells (field 1) appeared to emerge from the rhombic lip earlier than lateral hRPe cells (fields 2 and 3), we can further address the contribution by field 1 cells to the hCPe by extending our earlier presented temporal fate map of the *Wnt1::FlpeER*^{T2}+ rhombic lip (Fig. 2H,I) to late embryonic stages. Such studies would also define, for the first time, the production interval for hCPe.

Doubly transgenic embryos (*Wnt1::FlpeER^{T2}; Flp-responsive PLAP indicator*) were given single doses of TAM at different embryonic stages, and the fate of rhombic lip descendant cells (PLAP+) determined with respect to hCPe at E16.5 (Fig. 5). Because neither hRPe nor hCPe cells expressed *FlpeER^{T2}*, but rather this expression only occurred in cells in the rhombic lip (Fig. 5A-F), and because no recombinase activity was detected in the absence of TAM (Fig. 5G-L, insets), then the presence of PLAP activity in E16.5 hCPe cells should reflect rhombic lip as the spatial site of origin, whereas the time of TAM administration should define a temporal window of emergence from the rhombic lip. Only following TAM administration at time points spanning E9.5-E13.5 were PLAP+ cells observed in the E16.5 hCPe (Fig. 5G-K). Earlier (E7.5 and E8.5) (see Fig. S3 in the supplementary material) and later

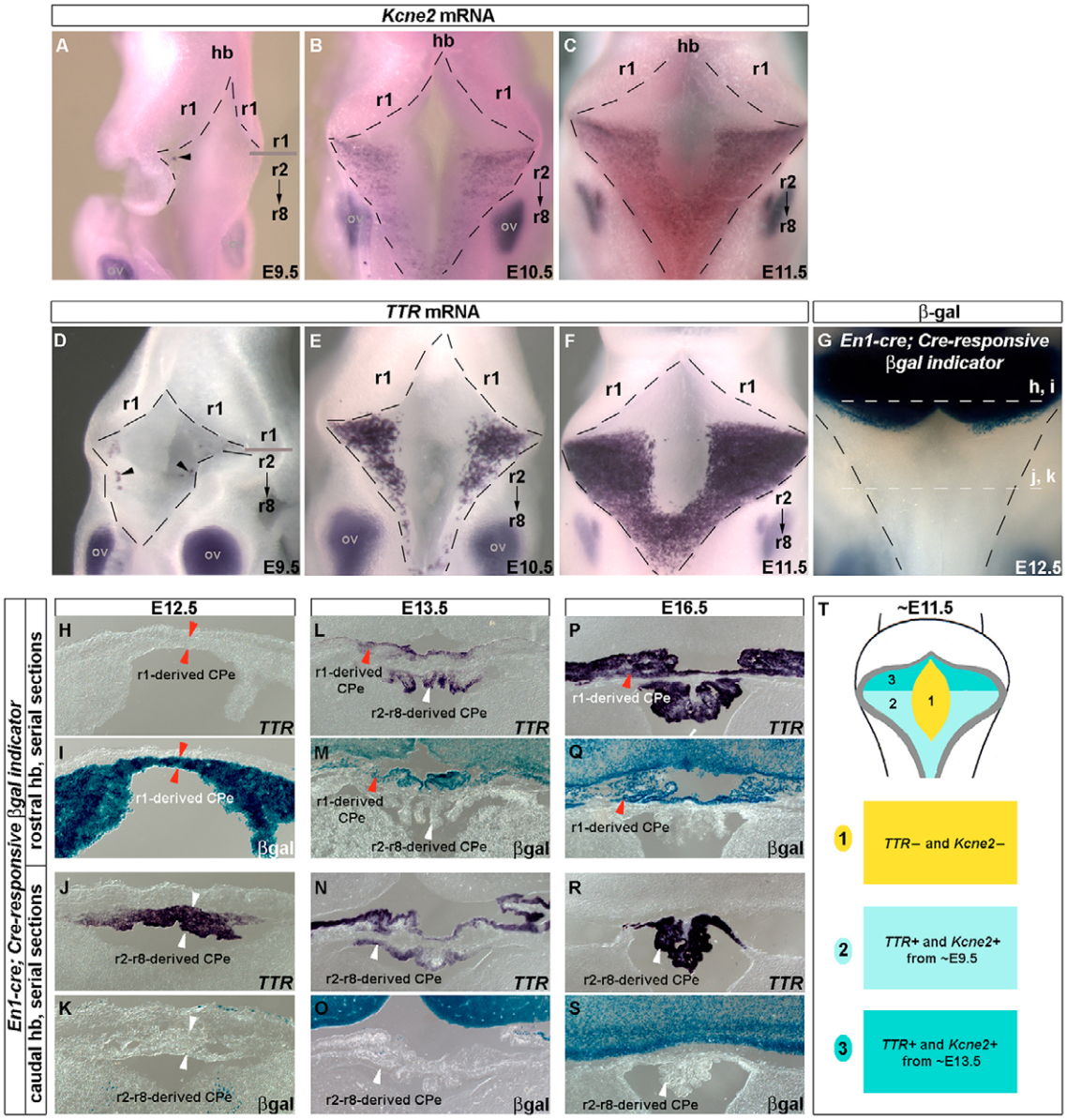

Fig. 4. Lateral roof plate derivatives from rhombomere 1 show a temporal lag in molecular fate as compared with those from rhombomeres 2-8. (**A-F**) Dorsal view of whole embryos processed to detect *Kcne2* mRNA (A-C) or *Ttr* mRNA (D-F). Broken lines demarcate the rhombic lip. *Kcne2* or *Ttr* transcripts were undetectable in the medial hindbrain roof plate epithelium (hRPe) field at all time points, but were readily detectable in the lateral hRPe field, except in those lateral cells derived from rhombomere 1 (r1). (**G**) Dorsal view of E12.5 doubly transgenic *En1::cre; Cre-responsive βgal indicator* embryos stained with X-gal to identify r1-derived cells. White broken lines indicate the levels of transverse sections shown in H-S (h,i,j,k); black broken lines demarcate the rhombic lip. (**H-S**) Serial transverse sections taken from doubly transgenic *En1::cre; Cre-responsive βgal indicator* embryos; one set was processed for *Ttr* mRNA detection, the other for X-gal detection of βgal. (H-K) Serial sections reveal that r1-derived βgal+ hCPe (red arrowheads) lacks *Ttr* activity at E12.5, whereas caudal (r2-r8-derived) βgal-negative (βgal–) hCPe (white arrowheads) is *Ttr*+. (L-S) By E13.5, all hCPe was *Ttr*+, whether derived from r1 (red arrowheads, βgal+) or from r2-r8 (white arrowheads, βgal-negative). (**T**) Schematic of three hRPe fields at ~E11.5: field 1 (yellow) is medially located, and is *Ttr*– and *Kcne2*–; field 2 (light blue) is laterally located but caudally derived (r2-r8), and is *Ttr*+ and *Kcne2*+ from ~E9.5 onwards; field 3 (dark blue) is laterally located but rostrally (r1)-derived, and is *Ttr*+ and *Kcne2*+ after E12.5 only. CPe, choroid plexus epithelium; hb, hindbrain; ov, otic vesicle.

(E14.5, Fig. 5L) administrations failed to result in detectable hCPe cell marking. These results suggest an hCPe production interval by the rhombic lip that spans ~E10-E14.

Corroborating this hCPe production interval are our results obtained following injection of the S-phase tracer BrdU. We performed analyses in doubly transgenic embryos (*Wnt1::cre; Cre-responsive βgal indicator*) to distinguish hCPe cells (nβgal+) from overlying mesenchymal and ectodermal cells. Co-localization of BrdU and nβgal was detectable following single BrdU injections between E10.5 and E13.5 (Fig. 5N-Q), with double-labeled hCPe cells most abundant following injection at E11.5-E12.5 (Fig. 5O,P). Few double-labeled cells were observed following BrdU injection at E9.5 (Fig. 5M) and none following injection at E14.5 (Fig. 5R). These findings predict a production interval spanning ~E9.5-E13.5, consistent with that determined by genetic inducible fate mapping. Together, these findings are consistent with a model whereby only lateral hRPe cells (fields 2 and 3) contribute to the hCPe. Interestingly, by ~E12.5, the epithelium tenting over the 4v appears morphologically to be hCPe and not hRPe (cuboidal versus pseudostratified, respectively). Therefore, at these later stages of development (~E12.5-E14), the rhombic lip might generate cells that differentiate directly into hCPe.

Differential response among rhombic lip lineages to ligand-independent activation of the Notch1 pathway

In many CNS regions, activation of the Notch signaling pathway in a cell sustains its capacity to proliferate (Louvi and Artavanis-Tsakonas, 2006) and thus imposes a progenitor cell-like identity. Multiple Notch genes are expressed in the ventricular zone of the hindbrain, including in the rhombic lip territory (Lindsell et al., 1996) (Fig. 6B). Using a *R26::stop-Notch1-ICD::IRES-nGFP* allele (Murtaugh et al., 2003), we expressed the intracellular domain of Notch1 (Notch1-ICD) – the constitutively active fragment – and a nuclear-localized green fluorescent protein (nGFP) in two different progenitor cell populations of the rhombic lip and their descendant lineages: (1) the dorsal-most progenitor cells in the rhombic lip

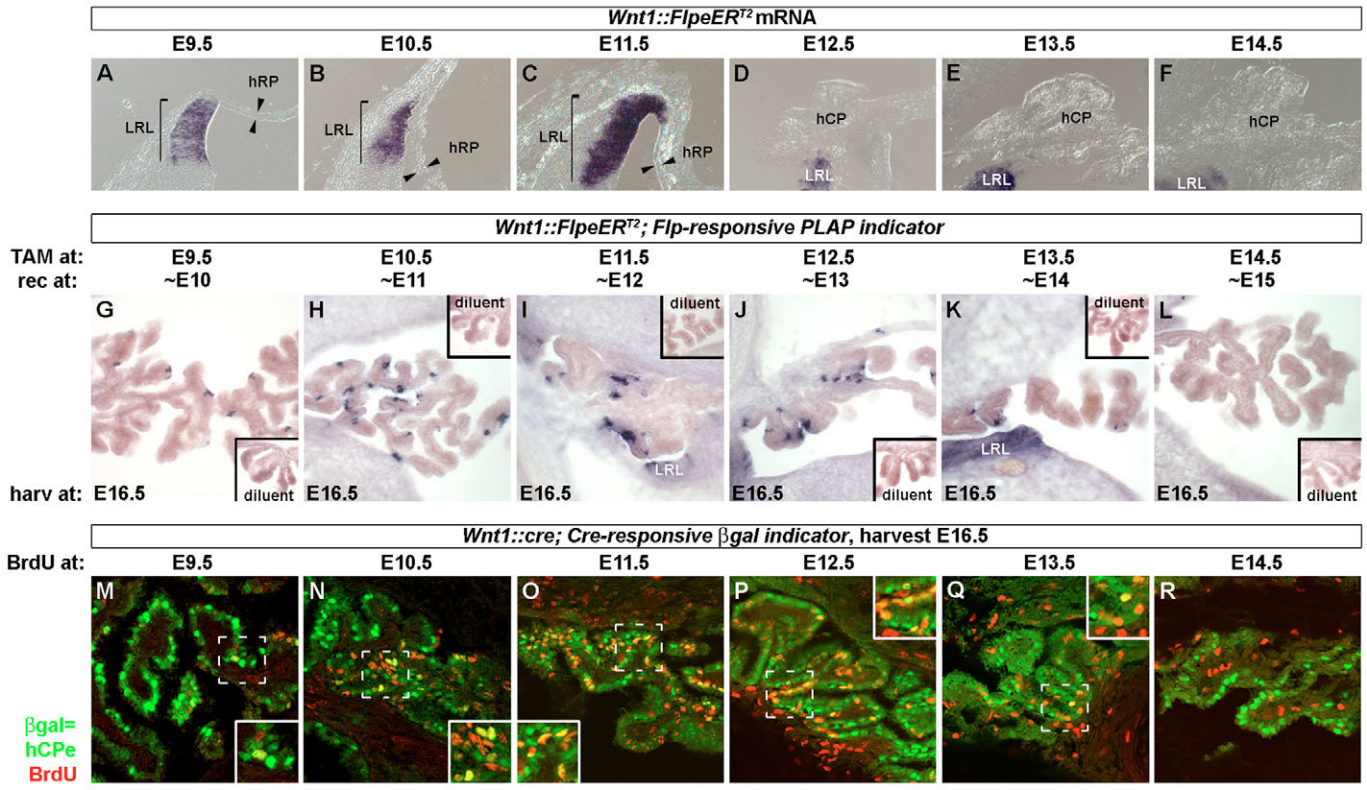

Fig. 5. Production of hindbrain choroid plexus epithelium begins at ~E9.5, peaks between ~E11 and E12, and terminates by ~E14. (**A-F**) Transverse sections through E9.5-E14.5 hindbrain that has been processed to detect *FlpeER^{T2}* mRNA show expression limited to the rhombic lip (vertical brackets in A-C), and absent from the hindbrain roof plate epithelium (hRPe, opposing black arrowheads) and hindbrain choroid plexus epithelium (hCPe). (**G-L**) Coronal sections processed for PLAP detection (dark precipitate) after harvest from E16.5 doubly transgenic *Wnt1::FlpeER^{T2}; R26::FRAP* embryos (*n*=9). Induction of FlpeER^{T2}-mediated recombination by tamoxifen (TAM) administration separates temporal cohorts of *Wnt1* (rhombic lip)-derived hCPe. (G) E9.5 TAM administration (recombination at ~E10 in the rhombic lip) resulted in a few labeled E16.5 hCPe cells. (H-J) TAM at E10.5 (recombination at ~E11), E11.5 (recombination at ~E12) or E12.5 (recombination at ~E13) resulted in numerous labeled cells in the E16.5 hCPe. (K,L) TAM administration at E13.5 (recombination at ~E14) resulted in few labeled hCPe cells (K), and none were present after administration at E14.5 (L). Insets in G-L reveal no PLAP activity when diluent alone was administered. (**M-R**) Coronal sections from doubly transgenic *Wnt1::cre; Cre-responsive βgal indicator* embryos, with βgal expression (green by immunodetection) distinguishing hCPe from underlying mesenchyme and vasculature, and red indicating BrdU incorporation, reflecting birthdate (time of single BrdU injection indicated above each panel). BrdU administered at either E9.5 or E14.5 showed very few co-labeled hCPe cells at E16.5 (M,R, respectively), whereas BrdU administered from E10.5 to E13.5 showed numerous co-labeled hCPe cells (N-Q). Insets show higher-power views of the boxed areas. rec, recombination time point; harv, harvest time point; hCP, hindbrain choroid plexus; LRL, lower rhombic lip.

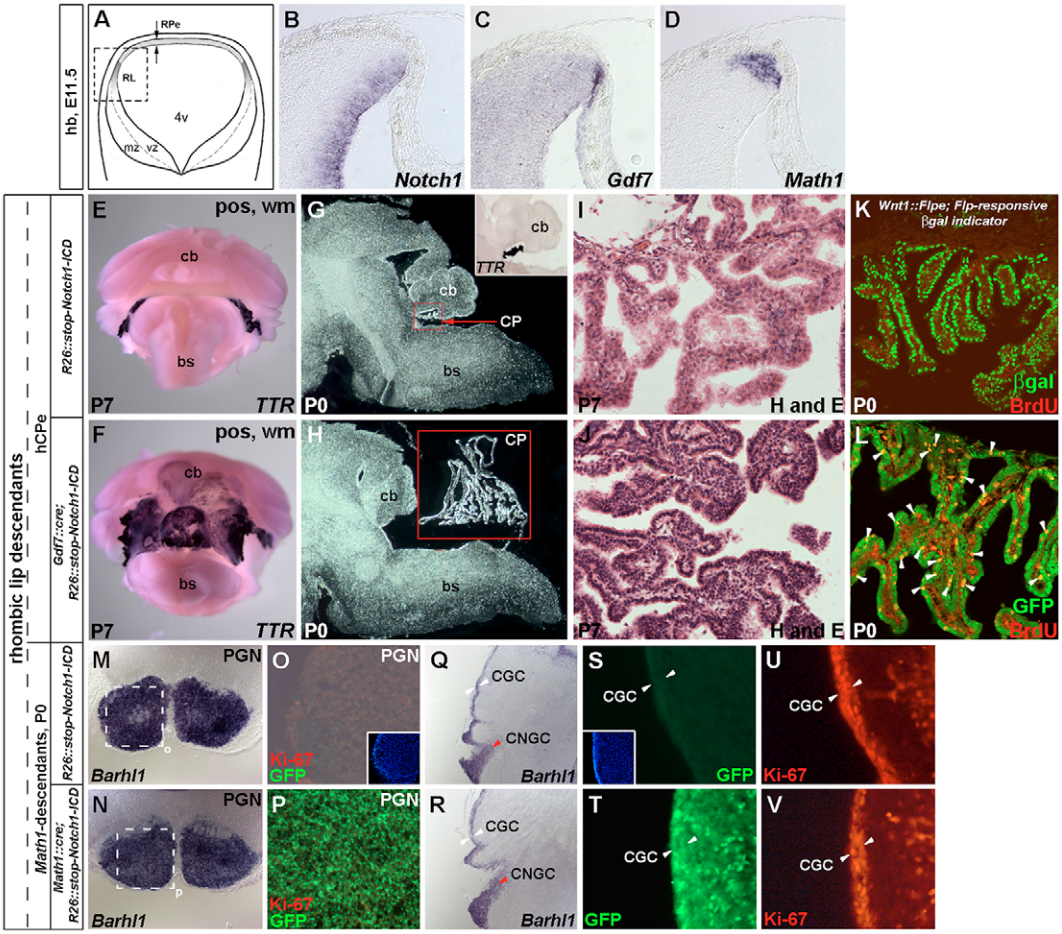

Fig. 6. Expression of activated Notch1 results in overproduction of hindbrain choroid plexus epithelium but not of other rhombic lip lineages. (**A**) Schematic of a transverse section through the hindbrain (hb), with the boxed area demarcating the region of the rhombic lip (RL) shown in B-D. (**B-D**) Detection of *Notch1*, *Gdf7* and *Math1* mRNA on E11.5 hindbrain serial sections. *Notch1* is expressed in the rhombic lip, but not in the hindbrain roof plate epithelium (hRPe); *Gdf7* is expressed in the distal tip of the rhombic lip and into the hRPe; and *Math1* is expressed in the rhombic lip ventral to the *Gdf7* expression territory. (**E-J**,**L**) Comparison of singly transgenic *R26::stop-Notch1-ICD::IRES-nGFP* (E,G,I) and doubly transgenic *Gdf7::cre; R26::stop-Notch1-ICD::IRES-nGFP* (F,H,J,L) brains. (E,F) Posterior (pos) whole-mount (wm) view of P7 brains processed for *Ttr* mRNA detection [hindbrain choroid plexus epithelium (hCPe) marker] showing enlarged hCPe in doubly transgenic tissue (F,H,J,L). (G,H) Sagittal sections showing enlarged postnatal day 0 (P0) hCPe (red boxes) and abnormal cerebellar architecture in doubly but not singly transgenic animals. Inset in G shows *Ttr*+ hCPe on a serial section to that shown in G. (I,J) Hematoxylin and Eosin staining at P7 shows abnormal cytoarchitecture of hCP in doubly transgenic tissues. (**K**) P0 doubly transgenic *Wnt1::Flpe; Flpe-responsive nβgal indicator* distinguishing hCPe (green by immunodetection of βgal) from underlying mesenchyme and vasculature. BrdU was injected into animals at P0, and tissue was harvested 2 hours later. BrdU immunodetection is shown in red. No co-labeled cells were found in wild-type hCPe, as shown. (L) Similar BrdU injection into doubly transgenic *Gdf7::cre; R26::stop-Notch1-ICD::IRES-nGFP* animals showed numerous co-labeled cells (arrowheads; GFP positivity identifying hCPe cells and expression of *Notch1-ICD*, and red indicating BrdU incorporation as a measure of proliferation). (**M-V**) Comparison of singly transgenic *R26::stop-Notch1-ICD::IRES-nGFP* and doubly transgenic *Math1::cre; R26::stop-Notch1-ICD::IRES-nGFP* brains. Coronal sections show no differences in size, relative cell density (*Barhl1* expression at P0) or proliferation (Ki-67 immunodetection at P5 shown in red; U,V) of *Math1*-derived rhombic lip lineages, including mossy fiber neurons of the pontine gray nucleus (PGN, M-P), cerebellar granule cell precursors (CGC, white arrowheads, Q-V) and granule cells of the cochlear nucleus (CNGC, red arrowheads, Q,R). GFP positivity (immunodetection shown in green) reflects expression of the *Notch1-ICD* transgene in PGN (O,P) and CGC (S,T). White boxes in M-N demarcate regions of the PGN shown in O,P. DAPI is shown in blue. 4v, fourth ventricle; bs, brainstem; cb, cerebellum; CP, choroid plexus; hb, hindbrain; mz, post-mitotic mantle zone; RPe, roof plate epithelium; vz, ventricular zone.

(*Gdf7*+) and their progeny cells – lateral hRPe and hCPe; or (2) *Math1* (*Atoh1*)-expressing progenitor cells of the rhombic lip and their progeny cells – including precerebellar mossy fiber neurons, cerebellar and cochlear nuclei granule cells (Farago et al., 2006; Landsberg et al., 2005; Wang et al., 2005).

Although these lineages demonstrated nGFP activity in doubly transgenic animals (Fig. 6L,P,T and data not shown), indicating expression of the *Notch1-ICD* transgene, only within the hRPe and hCPe lineages did we detect a proliferation response. On postnatal day (P)7, doubly transgenic *Gdf7::cre; R26::stop-Notch1-ICD::IRES-nGFP* mice showed substantial expansion of the hCPe (Fig. 6E,G singly versus Fig. 6F,H doubly transgenic); indeed, the cerebellum and midbrain appeared to be pushed forward as a consequence (Fig. 6H). Moreover, brain ventricles were expanded and CSF was in excess, reminiscent of hydrocephalus (Lindeman et al., 1998). In addition, each hCPe cell normally attaches to a

basement membrane (Thomas et al., 1988); by contrast, hCPe cells in doubly transgenic *Gdf7::cre; R26::stop-Notch1-ICD::IRES-nGFP* animals were found in disorganized piles (Fig. 6I,J), suggestive of a compromised blood-CSF barrier.

Given the association between Notch signaling and proliferation (Louvi and Artavanis-Tsakonas, 2006) together with the enlarged hCPe in doubly transgenic *Gdf7::cre; R26::stop-Notch1-ICD::IRES-nGFP* animals, we asked whether these hCPe cells had become mitotic. P0 doubly transgenic *Gdf7::cre; R26::stop-Notch1-ICD::IRES-nGFP* animals were pulsed with BrdU and 2 hours later hCPe cells were co-immunostained for GFP (marker for hCPe cells expressing *Notch1-ICD*) and BrdU. Approximately 20% of hCPe cells were co-labeled for GFP and BrdU following hCPe misexpression of Notch1-ICD and GFP (Fig. 6L); by contrast, no hCPe cells were co-labeled (Fig. 6K) in wild-type animals (doubly transgenic *Wnt1::Flpe; Flp-responsive ßgal indicator* animals; βgal identifies the hCPe and BrdU identifies cycling cells). These results (compare Fig. 6L and 6K) suggest that when *Notch1-ICD* is expressed, normally non-mitotic hCPe cells (Kappers et al., 1958; Knudsen, 1964; Li et al., 2002; Sturrock, 1979) proliferate.

To assay for *Notch1-ICD* effects in *Math1*+ rhombic lip-descendant cells, neurons in the pontine gray nucleus and granule cell precursors in the cerebellum of doubly transgenic *Math1::cre; R26::stop-Notch1-ICD::IRES-nGFP* animals were analyzed (Farago et al., 2006; Li et al., 2004). No gross changes were observed in either the area occupied by or the density of *Barhl1*+ cells – a marker for *Math1*-descendants (Fig. 6M,N and Q,R). Furthermore, neurons on route to or residing in the pontine gray nucleus showed no proliferation in response to Notch1-ICD (yet were robustly GFP+, indicating good expression of the *Notch1-ICD* transgene) (Fig. 6O,P). Cerebellar granule cell precursors expressing Notch1-ICD (GFP+) appeared to proliferate to the same extent as seen in littermate controls (Fig. 6S-V).

DISCUSSION

Here we present evidence for a model in which the hRPe is comprised of at least three spatiotemporal fields, differing in organization, proliferative state, order of emergence from the rhombic lip, and molecular profile of either the constituent cells and/or their parental cells. Only two of these hRPe fields appear to contribute to hCPe. We show that hCPe also receives contributions directly from the rhombic lip at late embryonic stages without seeming to transition through a morphologically hRPe-type intermediate. We define for the first time the temporal interval for hCPe production, revealing a surprisingly long period spanning ~E10-E14. Further, we show that the hCPe lineage appears unique among rhombic lip-derived lineages in that hCPe cells, which are normally non-mitotic, proliferate exuberantly in response to constitutive Notch1 signaling, whereas neuronal lineages arising from the *Math1*+ rhombic lip do not. These results are summarized schematically in Fig. 7.

Identification of distinct fields within the hindbrain roof plate

hRPe has been considered to serve two major roles: as a dorsal organizing center (Lee et al., 2000; Lee and Jessell, 1999; Liem, Jr et al., 1997; Millonig et al., 2000) and as an intermediate epithelium that transforms into CSF-producing hCPe (Thomas and Dziadek, 1993; Wilting and Christ, 1989). As an organizing center, the hRPe has been shown to influence dorsal neuroectoderm to express distinct sets of transcription factors at different DV positions, thereby establishing unique progenitor populations productive of different neuron subtypes. Evidence has emerged to support the possibility that the hRPe itself might differ along the AP axis (Awatramani et al., 2003; Chizhikov et al., 2006). Here, we show that the hRPe is heterogeneous along multiple dimensions, suggesting that, in addition to regulating hindbrain cell type production along the DV dimension, the hRPe might have the capacity to differentially influence hindbrain cell fate along the AP and temporal axes.

We show that the E11.5 hRPe comprises at least three fields distinguished by spatial, temporal, molecular and architectonic parameters (schematized in Fig. 2J, Fig. 3I, Fig. 4T). Field 1 cells occupy the dorsal midline. They emerge early from the rhombic lip (~E8-E9.5), arising from a *Wnt1*+ but *Gdf7*-negative (*Gdf7*–) progenitor cell population, and disperse extensively along the AP and DV axes, mixing among hRPe cells derived from different rhombomeric levels as well as among mesenchymal cells. Field 1 cells appear mitotic until ~E10.5.

By contrast, cells in fields 2 and 3 situate laterally and emerge from double-positive *Wnt1*+/*Gdf7*+ progenitor cells in the rhombic lip beginning at ~E9.5. Cells of fields 2 and 3 are non-mitotic, and those arising from different rhombomeric levels neither intermix nor do they mix with overlying mesenchyme. Thus, the adhesion properties of cells in fields 2 and 3 result in compartmentalization along both the AP and DV axes. Because r1-derived cells of field 2 can be distinguished molecularly from the rest of field 2 (derived from r2-r8), we have designated them as field 3. Transcripts detectable in field 2 starting at ~E9.5 and onward, such as *Ttr* and *Kcne2*, are detectable in field 3 after E12.5 only.

In the formation of hCPe – a non-mitotic structure – a linear developmental progression has been assumed, with the pseudostratified hRPe spreading out to become the monolayer cuboidal epithelium of the hCPe. This is thought to occur entirely through the conservative process of cell shape change. It appears that epithelial transformation is indeed an aspect of hCPe genesis, but involving only fields 2 and 3. Further, rhombic lip at later time points (~E12.5-E14) appeared to contribute directly to hCPe when hRPe seemed no longer present, suggesting that some hCPe cells probably arise without transforming through an hRPe intermediate or that the intermediate is short-lived.

Contribution to hCPe by field 1 is unlikely, because we failed to detect areas of hCPe that: (1) emerged from the rhombic lip between E8-E9.5 (as assayed by temporal genetic fate mapping as well as by BrdU birth-dating); and (2) were comprised of an admixture of cells derived from different rhombomeres. Rather, the hCPe appeared to be built from the rhombomere-based lineage-restricted compartments of fields 2 and 3 (Fig. 4M,Q) (Awatramani et al., 2003). Field 1 cells might be eliminated, although we did not detect apoptotic activity as assayed by TUNEL or Caspase 3 immunodetection (data not shown).

Although the fate of field 1 hRPe cells remains unknown, during embryogenesis they show similarities with roof plate cells of the spinal neural tube: field 1 hRPe cells emerge temporally from the rhombic lip coincident with the production of spinal roof plate cells (sRPe), both hRPe and sRPe situate along the dorsal midline, both cell types exhibit some degree of mitotic activity, and neither express *Ttr* or *Kcne2*. Additionally, cells either in field 1 hRPe or sRPe (but not hRPe fields 2 and 3) exhibit mixing with neighboring RPe cells. Thus, it is possible that field 1 hRPe cells conform better to what is thought of as roof plate, and that the hRPe cells in fields 2 and 3 might be better classified as postmitotic hCPe precursor

cells. We propose that, during embryogenesis, organizer function shifts from field 1 hRPe (perhaps 'true' roof plate) to fields 2 and 3 hRPe (incipient hCPe), and ultimately to the hCPe itself at late stages. It will be important to determine what regulates the production of these different fields. Regulators probably include differential signals emanating from mesenchyme overlying the hRPe versus incipient hCPe, as well as intrinsic molecular differences in rhombic lip progenitor cells over the course of development.

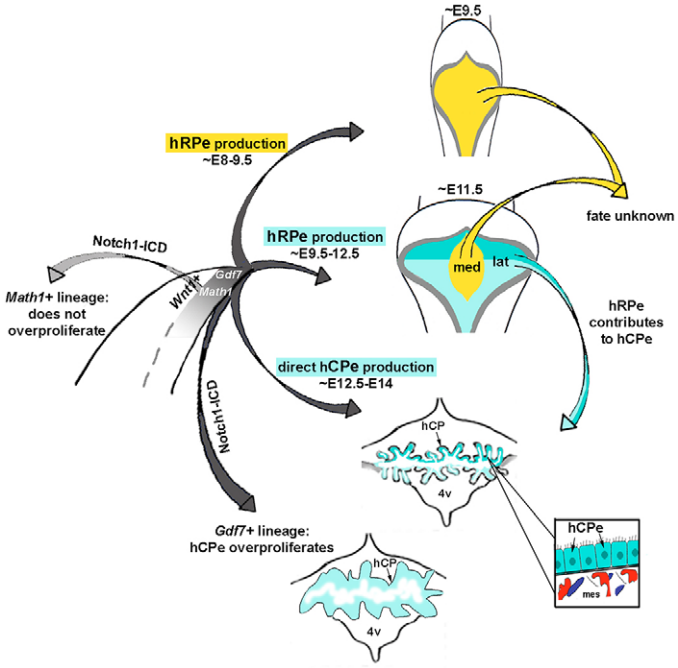

Fig. 7. Summary schematic of distinct subdivisions in the hindbrain roof plate, their differential contribution to the hindbrain choroid plexus and differential responses among rhombic lip lineages to activated Notch1. *Wnt1* mRNA in the rhombic lip is graded, with the highest expressers giving rise to hindbrain roof plate epithelium (hRPe) beginning at ~E8. These cells emerge from the rhombic lip and occupy the entire hRPe by ~E9.5 (yellow); they intermix in the anteroposterior (AP) and dorsoventral (DV) dimensions and are highly proliferative. Beginning at ~E9.25-E9.5, *Gdf7* expression starts in the dorsal-most progenitor cells in the rhombic lip and these progenitors give rise to hRPe (dark blue) that is compartmentalized in both the AP and DV dimensions, settles laterally and is non-mitotic immediately upon emerging from the rhombic lip. The medially located (yellow) hRPe cells have a history of *Wnt1* expression, whereas the laterally located (dark blue) hRPe cells have a history of both *Wnt1* and *Gdf7* expression. Caudally (r2-r8)-derived lateral hRPe (light blue) expresses *Ttr* and *Kcne2* from ~E9.5 onwards, whereas expression in rostrally (r1)-derived cells only occurs after E12.5. Beginning at ~E12.5, laterally located hRPe cells (light and dark blue) undergo cell shape changes to form the hindbrain choroid plexus epithelium (hCPe) (not drawn to scale). Medially located hRPe cells (yellow) do not appear to contribute to the hCPe. From ~E12.5 through to E14, *Gdf7*+ progenitors within the rhombic lip probably generate hCPe cells directly, without seeming to transition through an hRPe intermediate. At ~E14, the production interval for hCPe ceases. Ligand-independent activation of the Notch1 signaling pathway in the *Gdf7* lineage (the hRPe and hCPe lineage) results in overproliferation of hCPe. 4v, fourth ventricle; hCP, hindbrain choroid plexus; mes, mesenchymal cells.

Roof plate derived from r1 versus caudal rhombomeres differentially regulate their molecular expression

Although hRPe fields 2 and 3 both give rise to hCPe, they differ in their onset of expression of hCPe markers: *Ttr* and *Kcne2* mRNA are detectable in field 2 cells upon their emergence from the rhombic lip beginning at ~E9.5, remaining detectable into adulthood, whereas these mRNAs are detectable in field 3 after ~E12.5 only. What is the significance of this temporal lag in molecular expression between cells in field 3 versus 2? The hindbrain roof plate has been shown to be a source of signaling molecules that are important for regulating progenitor cells in the upper or cerebellar rhombic lip (Alder et al., 1999; Chizhikov et al., 2006), and this function is most likely served by immediately adjacent roof plate territory (i.e. r1-derived field 3). We studied whether the timing of molecular changes in field 3 might correspond with an event occurring in the cerebellar rhombic lip; for example, a shift in cell type production. Between ~E12.5 and E13.5, the cerebellar rhombic lip stops generating neurons destined for cerebellar nuclei and starts producing precursors of cerebellar granule cells (Machold and Fishell, 2005). Perhaps cells in field 3 remain less differentiated molecularly, less 'hCPe-like', in order to permit the cerebellar rhombic lip to first produce neurons destined for the cerebellar nuclei, and later become more 'hCPe-like' (reflected in the expression of *Ttr* and *Kcne2*) in order to induce production of cerebellar granule neurons by the cerebellar rhombic lip. It will be important to establish whether such regulation of cell type production is influenced by molecular changes occurring in field 3 and what actual field 3-derived factors might be responsible.

Field 3 cells did not emerge later from the rhombic lip than field 2 cells; therefore, events that control this delay in field 3 gene expression probably occur after constituent cells have emerged from the rhombic lip. The molecular boundary between fields 2 and 3 was sharp, coinciding with the r1-r2 boundary and latitude of hindbrain flexure. Future studies will involve assessing possible explanations for this exacting difference in molecular expression between fields 2 and 3, and whether, for example, the closely overlying mesenchyme situated above field 3 (rostral to hindbrain flexure) is different in its profile of cell-cell signaling molecules as compared to the mesenchyme situated above field 2 (caudal to hindbrain flexure).

Formation of the hindbrain choroid plexus epithelium is not simply a conservative transformation from pseudostratified to cuboidal cells

We present evidence that the interval for hCPe production spans from ~E10 to E14, with contributions arising via transformation of hRPe cells in fields 2 and 3, but not in field 1. Further, our data suggest that the rhombic lip makes a direct contribution to the hCPe at later stages. This model differs from the previously accepted view of a linear progression in development, in which the rhombic lip is the source of non-mitotic roof plate cells that transform to form hCPe in its entirety (Dohrmann, 1970; Dziegielewska et al., 2001; Kappers, 1955; Sturrock, 1979; Thomas and Dziadek, 1993; Wilting and Christ, 1989). In this conservative model, the increased epithelial surface area crucial to hCPe function arises solely from changes in cell shape – a densely packed pseudostratified RPe spreads out into a simple monolayered cuboidal epithelium. Here, we show that the addition of new cells to the hCPe by the rhombic lip contributes to its expansion.

Selective ability of hindbrain *Gdf7*-derived cells to respond to constitutively active Notch1 signaling

We show that the normally non-mitotic hCPe lineage proliferates exuberantly in response to constitutive expression of the intracellular domain of Notch1 (*Notch1-ICD*), and thus presumably in response to constitutive Notch1 signaling. By contrast, the rhombic lip-derived lineages characterized by early *Math1* expression did not proliferate abnormally in response to *Notch1-ICD*. Are hCPe cells somehow poised to re-enter the cell cycle? In adult rats, quiescent choroid plexus epithelium (CPe) cells in all three ventricles gain BrdU reactivity by 2 hours post an ischemic event, with a subset of these cells expressing neuronal nuclear antigen (NeuN) and glial fibrillary acidic protein (GFAP); this has led to the conclusion that the choroid plexus might harbor neural stem cells (Li et al., 2002). Transplantation studies in which 4v choroid plexus cells were grafted into damaged rat spinal cord showed a gain in GFAP immunoreactivity and that at least some of the choroid plexus cells differentiated into astrocytes (Kitada et al., 2001). These stem cell-like features might be further reflected in our observation of hCPe proliferation in response to *Notch1-ICD*. Interestingly, *Notch3-ICD* introduced into periventricular cells via retroviral injection caused what were described as hindbrain choroid plexus tumors (Dang et al., 2006).

In summary, we have shown that the hRPe is not a homogeneous cell population. Rather, it can be subdivided into at least three unique fields – cells in only two of these three fields contribute to the hCPe. We identify the temporal interval for hindbrain choroid plexus epithelium production and propose a novel process for its development. Our finding of spatial (mediolateral and anteroposterior), temporal and molecular differences among hRPe fields supports the model whereby the hindbrain roof plate and choroid plexus epithelium are complex structures that might exert patterning influences along AP and temporal, in addition to DV, axes. Our studies also highlight a unique property of rhombic lip-descendant hCPe cells, as compared with rhombic lip-descendant (*Math1*-descendant) neurons, for example, in their ability to proliferate in response to ligand-independent Notch1 signaling. This finding might have important implications for understanding choroid plexus tumor biology as well as the potential application of hCPe cells in CNS therapeutics and drug delivery.

We acknowledge R. Awatramani for helpful discussions; A. Farago, H. DiPietrantonio, C. Nielsen and J. Mai for technical assistance; T. Jessell, A. Joyner, D. Melton, D. Rowitch and S. Schneider-Maunoury for mouse strains; C. Cepko, A. McMahon, K. Millen, C. Tabin and C. Walsh for riboprobe templates. Support for S.M.D. and N.L.H. include NIH/R21/HD044915; P01/HD0363379 and R01/NS047750.

Supplementary material

Supplementary material for this article is available at http://dev.biologists.org/cgi/content/full/134/19/3449/DC1

References

Alder, J., Lee, K. J., Jessell, T. M. and Hatten, M. E. (1999). Generation of cerebellar granule neurons in vivo by transplantation of BMP-treated neural progenitor cells. *Nat. Neurosci.* **2**, 535-540.

Awatramani, R., Soriano, P., Mai, J. J. and Dymecki, S. (2001). An Flp indicator mouse expressing alkaline phosphatase from the ROSA26 locus. *Nat. Genet.* **29**, 257-259.

Awatramani, R., Soriano, P., Rodriguez, C., Mai, J. J. and Dymecki, S. M. (2003). Cryptic boundaries in roof plate and choroid plexus identified by intersectional gene activation. *Nat. Genet.* **35**, 70-75.

Chai, Y., Jiang, X., Ito, Y., Bringas, P., Jr, Han, J., Rowitch, D. H., Soriano, P., McMahon, A. P. and Sucov, H. M. (2000). Fate of the mammalian cranial neural crest during tooth and mandibular morphogenesis. *Development* **127**, 1671-1679.

Chan, W., Tam, W., Yung, K., Cheung, C., Sham, M. and Copp, A. (2003). Tracking down the migration of mouse neural crest cells. *Neuroembryology* **2**, 9-17.

Chizhikov, V. V. and Millen, K. J. (2004a). Control of roof plate development and signaling by Lmx1b in the caudal vertebrate CNS. *J. Neurosci.* **24**, 5694-5703.

Chizhikov, V. V. and Millen, K. J. (2004b). Mechanisms of roof plate formation in the vertebrate CNS. *Nat. Rev. Neurosci.* **5**, 808-812.

Chizhikov, V. V., Lindgren, A. G., Currle, D. S., Rose, M. F., Monuki, E. S. and Millen, K. J. (2006). The roof plate regulates cerebellar cell-type specification and proliferation. *Development* **133**, 2793-2804.

Dang, L., Fan, X., Chaudhry, A., Wang, M., Gaiano, N. and Eberhart, C. G. (2006). Notch3 signaling initiates choroid plexus tumor formation. *Oncogene* **25**, 487-491.

Dohrmann, G. J. (1970). The choroid plexus: a historical review. *Brain Res.* **18**, 197-218.

Dziegielewska, K. M., Ek, J., Habgood, M. D. and Saunders, N. R. (2001). Development of the choroid plexus. *Microsc. Res. Tech.* **52**, 5-20.

Emerich, D. F., Skinner, S. J., Borlongan, C. V., Vasconcellos, A. V. and Thanos, C. G. (2005). The choroid plexus in the rise, fall and repair of the brain. *BioEssays* **27**, 262-274.

Farago, A. F., Awatramani, R. B. and Dymecki, S. M. (2006). Assembly of the brainstem cochlear nuclear complex is revealed by intersectional and subtractive genetic fate maps. *Neuron* **50**, 205-218.

Fraser, S., Keynes, R. and Lumsden, A. (1990). Segmentation in the chick embryo hindbrain is defined by cell lineage restrictions. *Nature* **344**, 431-435.

Harms, P. J., Tu, G. F., Richardson, S. J., Aldred, A. R., Jaworowski, A. and Schreiber, G. (1991). Transthyretin (prealbumin) gene expression in choroid plexus is strongly conserved during evolution of vertebrates. *Comp. Biochem. Physiol.* **99B**, 239-249.

Herbert, J., Wilcox, J. N., Pham, K. T., Fremeau, R. T., Jr, Zeviani, M., Dwork, A., Soprano, D. R., Makover, A., Goodman, D. S., Zimmerman, E. A. et al. (1986). Transthyretin: a choroid plexus-specific transport protein in human brain. The 1986 S. Weir Mitchell award. *Neurology* **36**, 900-911.

Hunter, N. L., Awatramani, R. B., Farley, F. W. and Dymecki, S. M. (2005). Ligand-activated Flpe for temporally regulated gene modifications. *Genesis* **41**, 99-109.

Kappers, J. A. (1955). The development of the paraphysis cerebri in man with comments on its relationship to the intercolumnar tubercle and its significance for the origin of cystic tumors in the third ventricle. *J. Comp. Neurol.* **102**, 425-509.

Kappers, J. A., Ten Kate, I. and De Bruyn, H. J. (1958). On mast cells in the choroid plexus of the axolotl (Ambystoma mex.). *Z. Zellforsch. Mikrosk. Anat.* **48**, 617-634.

Kimmel, R. A., Turnbull, D. H., Blanquet, V., Wurst, W., Loomis, C. A. and Joyner, A. L. (2000). Two lineage boundaries coordinate vertebrate apical ectodermal ridge formation. *Genes Dev.* **14**, 1377-1389.

Kitada, M., Chakrabortty, S., Matsumoto, N., Taketomi, M. and Ide, C. (2001). Differentiation of choroid plexus ependymal cells into astrocytes after grafting into the pre-lesioned spinal cord in mice. *Glia* **36**, 364-374.

Knudsen, P. A. (1964). Mode of growth of the choroid plexus in mouse embryos. *Acta Anat. Basel* **57**, 172-182.

Landsberg, R. L., Awatramani, R. B., Hunter, N. L., Farago, A. F., DiPietrantonio, H. J., Rodriguez, C. I. and Dymecki, S. M. (2005). Hindbrain rhombic lip is comprised of discrete progenitor cell populations allocated by Pax6. *Neuron* **48**, 933-947.

Lee, K. J. and Jessell, T. M. (1999). The specification of dorsal cell fates in the vertebrate central nervous system. *Annu. Rev. Neurosci.* **22**, 261-294.

Lee, K. J., Dietrich, P. and Jessell, T. M. (2000). Genetic ablation reveals that the roof plate is essential for dorsal interneuron specification. *Nature* **403**, 734-740.

Li, S., Qiu, F., Xu, A., Price, S. M. and Xiang, M. (2004). Barhl1 regulates migration and survival of cerebellar granule cells by controlling expression of the neurotrophin-3 gene. *J. Neurosci.* **24**, 3104-3114.

Li, Y., Chen, J. and Chopp, M. (2002). Cell proliferation and differentiation from ependymal, subependymal and choroid plexus cells in response to stroke in rats. *J. Neurol. Sci.* **193**, 137-146.

Liem, K. F., Jr, Tremml, G., Roelink, H. and Jessell, T. M. (1995). Dorsal differentiation of neural plate cells induced by BMP-mediated signals from epidermal ectoderm. *Cell* **82**, 969-979.

Liem, K. F., Jr, Tremml, G. and Jessell, T. M. (1997). A role for the roof plate and its resident TGFbeta-related proteins in neuronal patterning in the dorsal spinal cord. *Cell* **91**, 127-138.

Lindeman, G. J., Dagnino, L., Gaubatz, S., Xu, Y., Bronson, R. T., Warren, H. B. and Livingston, D. M. (1998). A specific, nonproliferative role for E2F-5 in choroid plexus function revealed by gene targeting. *Genes Dev.* **12**, 1092-1098.

Lindsell, C. E., Boulter, J., diSibio, G., Gossler, A. and Weinmaster, G. (1996). Expression patterns of Jagged, Delta1, Notch1, Notch2, and Notch3 genes identify ligand-receptor pairs that may function in neural development. *Mol. Cell. Neurosci.* **8**, 14-27.

Louvi, A. and Artavanis-Tsakonas, S. (2006). Notch signalling in vertebrate neural development. *Nat. Rev. Neurosci.* **7**, 93-102.

Lundquist, A. L., Turner, C. L., Ballester, L. Y. and George, A. L., Jr (2006).

Expression and transcriptional control of human KCNE genes. *Genomics* **87**, 119-128.
Machold, R. and Fishell, G. (2005). Math1 is expressed in temporally discrete pools of cerebellar rhombic-lip neural progenitors. *Neuron* **48**, 17-24.
Manzanares, M. and Krumlauf, R. (2000). Developmental biology. Raising the roof. *Nature* **403**, 720-721.
Matei, V., Pauley, S., Kaing, S., Rowitch, D., Beisel, K. W., Morris, K., Feng, F., Jones, K., Lee, J. and Fritzsch, B. (2005). Smaller inner ear sensory epithelia in Neurog 1 null mice are related to earlier hair cell cycle exit. *Dev. Dyn.* **234**, 633-650.
Millen, K. J., Millonig, J. H. and Hatten, M. E. (2004). Roof plate and dorsal spinal cord dl1 interneuron development in the dreher mutant mouse. *Dev. Biol.* **270**, 382-392.
Millonig, J. H., Millen, K. J. and Hatten, M. E. (2000). The mouse Dreher gene Lmx1a controls formation of the roof plate in the vertebrate CNS. *Nature* **403**, 764-769.
Murtaugh, L. C., Stanger, B. Z., Kwan, K. M. and Melton, D. A. (2003). Notch signaling controls multiple steps of pancreatic differentiation. *Proc. Natl. Acad. Sci. USA* **100**, 14920-14925.
Redzic, Z. B., Preston, J. E., Duncan, J. A., Chodobski, A. and Szmydynger-Chodobska, J. (2005). The choroid plexus-cerebrospinal fluid system: from development to aging. *Curr. Top. Dev. Biol.* **71**, 1-52.
Segal, M. B. (2000). The choroid plexuses and the barriers between the blood and the cerebrospinal fluid. *Cell. Mol. Neurobiol.* **20**, 183-196.
Soriano, P. (1999). Generalized lacZ expression with the ROSA26 Cre reporter strain. *Nat. Genet.* **21**, 70-71.
Sturrock, R. R. (1979). A morphological study of the development of the mouse choroid plexus. *J. Anat.* **129**, 777-793.
Thomas, T. and Dziadek, M. (1993). Capacity to form choroid plexus-like cells in vitro is restricted to specific regions of the mouse neural ectoderm. *Development* **117**, 253-262.
Thomas, T., Power, B., Hudson, P., Schreiber, G. and Dziadek, M. (1988). The expression of transthyretin mRNA in the developing rat brain. *Dev. Biol.* **128**, 415-427.
Voiculescu, O., Charnay, P. and Schneider-Maunoury, S. (2000). Expression pattern of a Krox-20/Cre knock-in allele in the developing hindbrain, bones, and peripheral nervous system. *Genesis* **26**, 123-126.
Wang, V. Y., Rose, M. F. and Zoghbi, H. Y. (2005). Math1 expression redefines the rhombic lip derivatives and reveals novel lineages within the brainstem and cerebellum. *Neuron* **48**, 31-43.
Wilting, J. and Christ, B. (1989). An experimental and ultrastructural study on the development of the avian choroid plexus. *Cell Tissue Res.* **255**, 487-494.
Zervas, M., Millet, S., Ahn, S. and Joyner, A. L. (2004). Cell behaviors and genetic lineages of the mesencephalon and rhombomere 1. *Neuron* **43**, 345-357.
Zhao, Q., Eberspaecher, H., Lefebvre, V. and De Crombrugghe, B. (1997). Parallel expression of Sox9 and Col2a1 in cells undergoing chondrogenesis. *Dev. Dyn.* **209**, 377-386.